**I J C T A**, 10(5) 2017, pp. 157-163


# Fully Controlled H-Bridge Converter Based IM Control with 12-Sided Polygonal SVPWM

**B. Swaroopa*** **and T. Teja Sreenu***

***Abstract:*** This paper defines a H-bridge converter topology with dodecagonal SVPWM controller for speed control of induction machine. This controller can suppress that of $6n \pm 1$ ($n$ = odd) harmonics component from system fundamental voltage and current with all ranges of modulation index. The H-bridge converter consist of full converter, The controller placed at both ends of the machine with different voltage levels. By the use of H-bridge topology the system performance is increased and power handling capability also increases.

***Index Terms:*** Dodecagonal space vectors, H-bridge, multilevel inverters, induction machine, SVPWM.

## 1. INTRODUCTION

Now a day's world industrialization increases day to day. Due to this utilization of variable drives increases to a greater extent, for this the research is going on implementation of effective controllers for power conversion with high efficiency. In basic level 2 level converters are used for power conversion. The major disadvantages are extended stress on power electronic devices, high loses and the harmonic content presented in output fundamental wave is greater extent. To compensate this disadvantages multi level converters are implemented. The switching voltage stress are less due to distributed devices, switching frequency is less compared to conventional 2level converters and THD content presented in fundamental wave is less due to step levels in its output wave. Different types of multilevel converters are Neutral point clamped converter, flying capacitor, H-Bridge, cascade and modular multilevel converters. Basically synchronous PWM technique is preferred for pulse generation, it can mitigate sub-harmonic generation. Due to this temperature rise is reduced to a considerable extent. This combination is used preferably in high power applications [1]–[9]. Here H-Bridge full controlled converters are used to control the induction motor excitation. The open ended type of induction motor is used [10, 11].

The combination of multilevel converter with SPWM imposes low frequency harmonics like $5^{th}$, $7^{th}$ and $9^{th}$. It affects motor current control to greater extent. To avid or to reduce this harmonics polygonal pulse width generation is used. 12 sided polygonal (dodecagonal) PWM is implemented to compensate above mentioned problems. The dodecagonal inverter can suppress the low frequency harmonics. That is it eliminates $6n \pm 1$ ($n$ = 1, 3, … odd) harmonic components over all modulation ranges [14]. The carrier based dodecagonal pulse width modulation used the full bridge type H-bridge inverter is used due to this the current control is smoothen and low frequency harmonics are eliminated. Hear the sampled type carrier is taken for timing calculation it can speed up the process compared to conventional case.

## 2. INVERTER POWER STAGE AND SPACE-VECTOR DIAGRAMS

The test system simulation model is as shown in Figure 2. H-Bridge inverter based IM drive with dodecagonal SVPWM. The two end voltages are at different level.

Every phase have two bridges, the each bridge excited with an voltage of 0.366 kVdc. The cells/ bridges in each phase can produce three levels one output is super impose with others output. The levels

* K.L. University. *Email: bezawadaswaroopa@gmail.com and tejasreenu.tadivaka@kluniversity.in*

are +kVdc, 0 and −kVdc in its output. The switching stages and corresponding voltages are shown in Table 1.

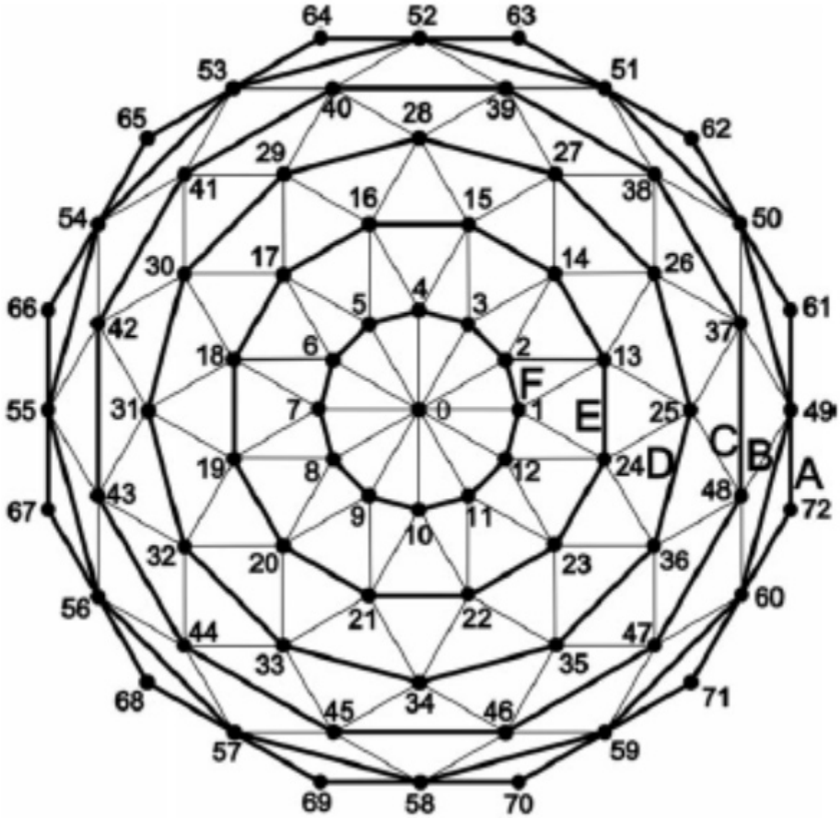


**Figure 1: 12 sided polygonal SVPWM for H-Bridge inverter**

The space vectors formed by the combinations of all the levels of pole voltages are calculated. The switching stages and patterns are shown in Figure 2. The radii of dodecagon is $r_i$ ($i$ = 1 to 6), with $i$ = 1. The ratio of radii's are $r_1 : r_2 : r_3 : r_4 : r_5 : r_6 = 1 : \cos(\pi/12) : \cos(2\pi/12) : \cos(3\pi/12) : \cos(4\pi/12) : \cos(5\pi/12)$. The spanning of the 0° to 30°, 30° to 60°.

The variable $k$ have significant preference in calculation of ratio of voltages. The maximum voltage during 12 step dodecagonal converter (0.659 × 2.45 kVdc) = 1.615 kVdc.

The rotar side dc voltage value taken is 0.37 Vdc = 1.615 kVdc, and hence, $k$ = 0.394, therefore

$$\begin{bmatrix} v_{\text{phA}} \\ v_{\text{phB}} \end{bmatrix} = \frac{1}{3}\begin{bmatrix} 2 & -1 & -1 \\ -1 & 2 & -1 \\ 1 & 1 & 2 \end{bmatrix}\begin{bmatrix} v_{\text{AN}} \\ v_{\text{BN}} \\ v_{\text{CN}} \end{bmatrix} \tag{1}$$

The resultant space vectors are defined as,

$$\text{V}_{\text{R}} = v_{\text{phA}} + v_{\text{phB}}e^{j2\pi/3} + v_{\text{phC}}e^{-\frac{j2\pi}{3}} \tag{2}$$

The two side voltages are 0.394 $\text{V}_{dc}$ and 0.144 Vdc. The H-bridge pulse generator modulation is extended to $m$ = 0.906 and linear modulation increased to $m$ = 0.966 [14].

The voltage states are shown in the Table 1. The switching stages and state of operation are explained based on that table.

**Table 1**
**Different switching combinations for different levels of pole voltage**

| *Magnitude (kVdc)* | *Level* | *S1* | *S2* | *S3* | *S7* | *VC1 (kVdc)* | *VC2 (kVdc)* |
|---|---|---|---|---|---|---|---|
| 1.366 | 4 | 0 | 1 | 0 | 1 | 1 | 0.366 |
| 1 | 3 | 0 | 1 | 0 | 0 | 1 | 0 |
| | | 0 | 1 | 1 | 1 | | |
| 0.634 | 2 | 0 | 1 | 1 | 0 | 1 | –0366 |
| 0.366 | 1 | 1 | 1 | 0 | 1 | 0 | 0.366 |
| | | 0 | 0 | 0 | 1 | | |
| 0 | 0 | 0 | 0 | 0 | 0 | 0 | 0 |
| | | 0 | 0 | 1 | 1 | | |
| | | 1 | 1 | 0 | 0 | | |
| | | 1 | 1 | 1 | 1 | | |
| –0.366 | –1 | 0 | 0 | 1 | 0 | 0 | –0.366 |
| | | 1 | 1 | 1 | 0 | | |
| –0.634 | –2 | 1 | 0 | 0 | 1 | –1 | –0.366 |
| –1 | –3 | 1 | 0 | 0 | 0 | –1 | 0 |
| | | 1 | 0 | 1 | 1 | | |
| –1.366 | –4 | 1 | 0 | 1 | 0 | –1 | –0.366 |

## 3. SWITCHING STAGES

The individual switching stages are shown in switching cycle, the timing calculations are define in [8], [9]. The switching stages are shown in Figure 3. Total three vectors are taken for three phases. The vectors one from type 1 and two vectors from 2nd polygon and vice-versa. Let the sectors be numbered from 1 to 6 in anticlockwise direction starting from the axis of phase-A winding (see Figure 2). We can identify the sectors from the sampled amplitudes of the reference voltage waveform. For example, if $|V_a| > |V_b| > |V_c|$ $\Rightarrow$ Sector 1. Further, the timings of the active vectors for the two-level hexagonal space-vector modulation $T_{1\ Hex}$ and $T_{2\ Hex}$ for a sector can also be computed [21].

For odd numbered sectors
$$\begin{bmatrix} T_{1\,Hex} \\ T_{2\,Hex} \end{bmatrix} = \frac{T_s}{\left| V_{1\,Hex} \right|} \begin{bmatrix} V_{max} - V_{mid} \\ V_{mid} - V_{min} \end{bmatrix}$$

For even numbered sectors
$$\begin{bmatrix} T_{1\,Hex} \\ T_{2\,Hex} \end{bmatrix} = \frac{T_s}{\left| V_{1\,Hex} \right|} \begin{bmatrix} V_{mid} - V_{min} \\ V_{max} - V_{mid} \end{bmatrix}$$

Odd sector switching with diff pattern is
$$\begin{bmatrix} T_{1\,Dod} \\ T_{2\,Dod} \end{bmatrix} = \begin{bmatrix} 1 & -1 \\ 0 & \sqrt{3} \end{bmatrix} \begin{bmatrix} T_{1\,Hex} \\ T_{2\,Hex} \end{bmatrix}$$

End Fordod-sector 2
$$\begin{bmatrix} T_{1\,Dod} \\ T_{2\,Dod} \end{bmatrix} = \begin{bmatrix} \sqrt{3} & -1 \\ 0 & 1 \end{bmatrix} \begin{bmatrix} T_{1\,Hex} \\ T_{2\,Hex} \end{bmatrix}$$

For 15° the switching is
$$\begin{bmatrix} T_{1\,Dod\,15} \\ T_{2\,Dod\,15} \end{bmatrix} = \begin{bmatrix} 0.5176 & -0.5176 \\ 0.5176 & \sqrt{2} \end{bmatrix} \begin{bmatrix} T_{1\,Dod} \\ T_{2\,Dod} \end{bmatrix}$$

When the reference vector is in the dod-subsector 2. The timings for the corresponding 15° rotated dodecagon vectors are $\begin{bmatrix} T_{1\,Dod\,15} \\ T_{2\,Dod\,15} \end{bmatrix} = \begin{bmatrix} \sqrt{2} & 0.5176 \\ -0.5176 & 0.5176 \end{bmatrix} \begin{bmatrix} T_{1\,Dod} \\ T_{2\,Dod} \end{bmatrix}$

The timings with voltage considerations is

$$T'_0 = \frac{|V_1|(T_1 + T_2) - |V_2|T_S}{|V'_0| - |V'_2|\cos(15)}\cos(15)$$

$$T'_1 = \frac{2|V_1|T_1\cos(15) - |V'_0|T'_0}{2|V'_1|\cos(15)}$$

$$T'_2 = \frac{2|V_2|T_2\cos(15) - |V'_0|T'_0}{2|V'_2|\cos(15)}$$

The switching stages are shown in Table 2. In each cell two devices are excited with same pulse for closing the circuit.

**Table 2**
**Switching stages**

| *Point* | *Switching States* | *Point* | *Switching States* | *Point* | *Switching States* |
|---|---|---|---|---|---|
| 0 | (000,0’0’0’), (000,1’1’1’), (000,’2’2’2), (111,0’0’0’), (111,1’1’1’), (111,’2’2’2’), (222,0’0’0’), (222,1’1’1’), (222,’2’2’2’) | 25 | (211,0,2’2’), (100,0’2’2’) | 50 | (210,0’1’2’) |
| 1 | (211,2’1’1’), (100,2’1’1), (100,1’0’0’) | 26 | (210,1’1’1’), (210,2’2’2’), (210,0’0’0’) | 51 | (220,1’1’2’), (220,0’0’1’) |
| 2 | (111,0’1’2’), (000,0’1’2’), (222, 0’1’2’) | 27 | (110,0’0’2’), (221,0’0’2’) | 52 | (120,1’0’2’) |
| 3 | (110,1’1’0), (110,2’2’1’), (221,2’2’1’) | 28 | (120,1’1’1’), (120,0’0’0’), (120,2’2’2’) | 53 | (020,1’0’1’), (020,2’1’2’) |
| 4 | (111,1’0’2’), (000,1’0’2’), (222,1’0’2’) | 29 | (010,2’0’2’), (121,2’0’2’) | 54 | (021,2’0’1’) |
| 5 | (010,0’1’0’), (010,1’2’1’), (121,0,1,0,), (121,1’2’1’) | 30 | (021,1’1’1’), (021,0’0’0’), (021,2’2’2’) | 55 | (022,2’1’1’), (022,1’0’0’) |
| 6 | (111,2’0’1’), (000,2’0’1’), (222,2’0’1’), | 31 | (011,2’0’0’), (122,2’0’0’) | 56 | (012,2’1’0’) |
| 7 | (011,0’1’1’), (011,1’2’2’), (122,0’1’1’), (122,1’2’2’) | 32 | (012,1’1’1’), (012,0’0’0’), (012,2’2’2’) | 57 | (002,1’1’0’), (022,2’2’1’) |
| 8 | (111,2’1’0), (000,2’1’0’), (222,2’1’0’) | 33 | (001,2’2’0’), (112,2’2’0’) | 58 | (102,1’2’0’) |
| 9 | (112,1’1’2’), (001,1’1’2’), (112,0’0’1’), (001,0’0’1’) | 34 | (102,1’1’1’), (102,0’0’0’), (102,2’2’2’) | 59 | (201,1’2’1’), (202,0’1’0’) |
| 10 | (111,1’2’0’), (000,1’2’0’), (222,1’2’0’) | 35 | (101,0’2’o’), (212,0’2’0’) | 60 | (201),0’2’1’) |
| 11 | (101,1’0’1’), (101,2’1’2’), (212,1’0’1’), (212,2’1’2’) | 36 | (201,1’1’1’), (201,0’0’0’), (201,2’2’2’) | 61 | (200,0’0’2’) |
| 12 | (111,0’2’1’), (000,0’2’1’), (222,0,2,1,) | 37 | (210,0’2’1’) | 62 | (220,0’2’2’) |
| 13 | (100,0’0’1’), (100,1’1’2’), (211,0’0’1’), (211,1’1’2’) | 38 | (210,1’0’2’) | 63 | (220,2’0’2’) |
| 14 | (110,1’2’2’), (110,0’1’1’), (221,1’2’2’) | 39 | (120,0’1’2’) | 64 | (020,0’0’2’) |
| 15 | (110,2’1’2’), (110,1’0’1’), (221,2’1’2’), (221,1’0’1’) | 40 | (120,2’0’1’) | 65 | (020,2’0’0’) |
| 16 | (121,0’0’1’), (121,1’1’2’), (010,0’0’1’), (010,1’1’2’) | 41 | (021,1’0’2’) | 66 | (022,2’0’2’) |

| *Point* | *Switching States* | *Point* | *Switching States* | *Point* | *Switching States* |
|---|---|---|---|---|---|
| 17 | (121,1’0’0’), (121,2’1’1’), (010,1’0’0’), (010,2’1’1’) | 42 | (021,1’0’2’) | 67 | (022,2’2’0’) |
| 18 | (001,2’1’2’), (011,1’0’1’), (122,2’1’2’), (122,1’0’1’) | 43 | (012,2’0’1’) | 68 | (002,2’0’0’0’) |
| 19 | (011,2’2’1’), (011,1’1’0’), (122,2’2’1’), (122,1’1’0’) | 44 | (012,1’2’0’) | 69 | (002,0’2’0’) |
| 20 | (112,1’0’0’), (112,2’1’1’), (001,1’0’0’), (001,2’1’1’) | 45 | (102,2’0’1’) | 70 | (202,2’2’0’) |
| 21 | (112,0’1’0’), (112,1’2’1’), (001,0’1’0’), (001,1’2’1’) | 46 | (102,0’2’1’) | 71 | (202,2’2’0’) |
| 22 | (101,2’2’1’), (101,1’1’2’), (212,1’1’0’), (212,1’1’0’) | 47 | (201,1’2’0’) | 72 | (200,0’2’0’) |
| 23 | (101,1’2’2’), (101,0’1’1’), (212,1’2’2’), (212,0’1’0’) | 48 | (201,0’1’2’) | | |
| 24 | (211,0’1’0’), (211,1’2’1’), (100,0’1’0’), (100,1’2’1’) | 49 | (200,0’1’1’), (200,1’2’1’) | | |

## 4. SIMULATION RESULTS

The simulation test system consists of Induction machine with *v/f* ratio control. The *v/f* ratio control can provide variable speed operation smoothly. The switching pulse can control the speed of the machine. The H-Bridge cells are connected in both sides of the machine. The rotor side converter switching reference is given with low frequency. The simulink block diagram is shown in Figure 2.

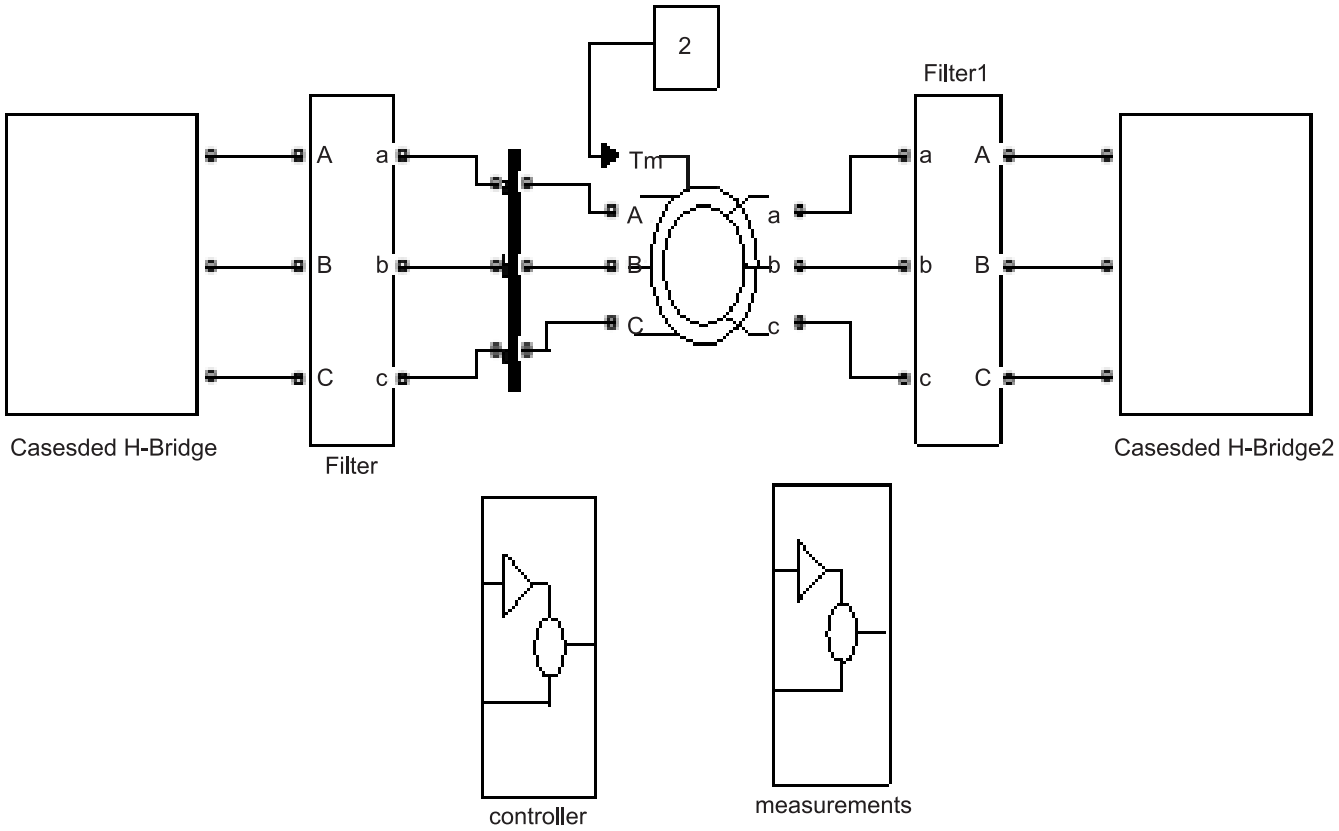


**Figure 2: H-Bridge inverter based IM drive with dodecagonal SVPWM**

The converter output voltage and currents are shown in Figure 3 and Figure 4.

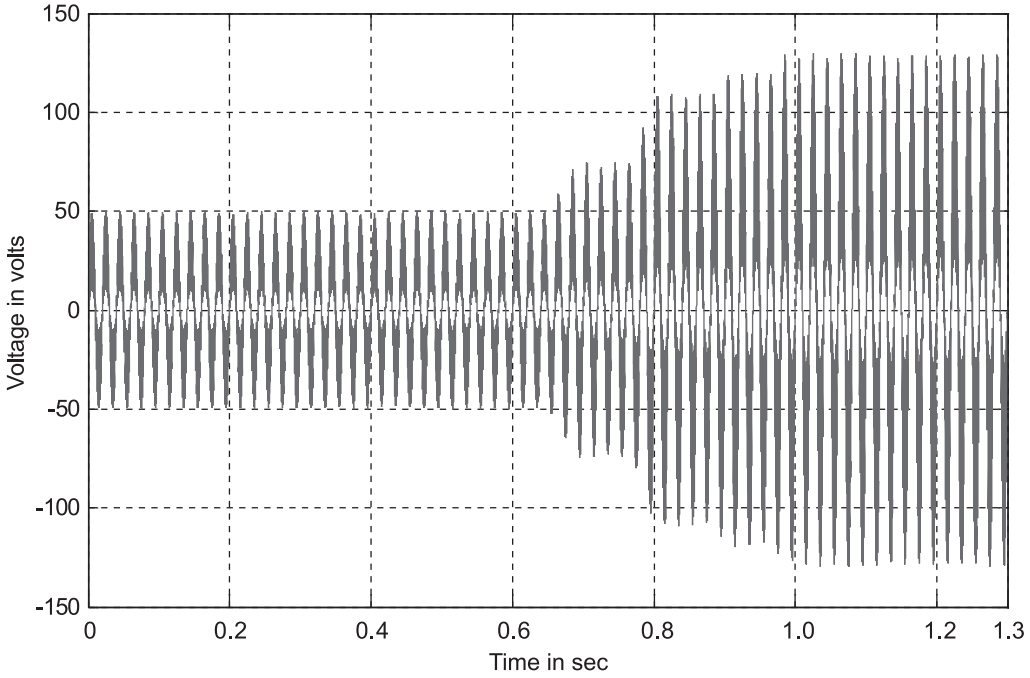


**Figure 3: Voltage of stator side converter**

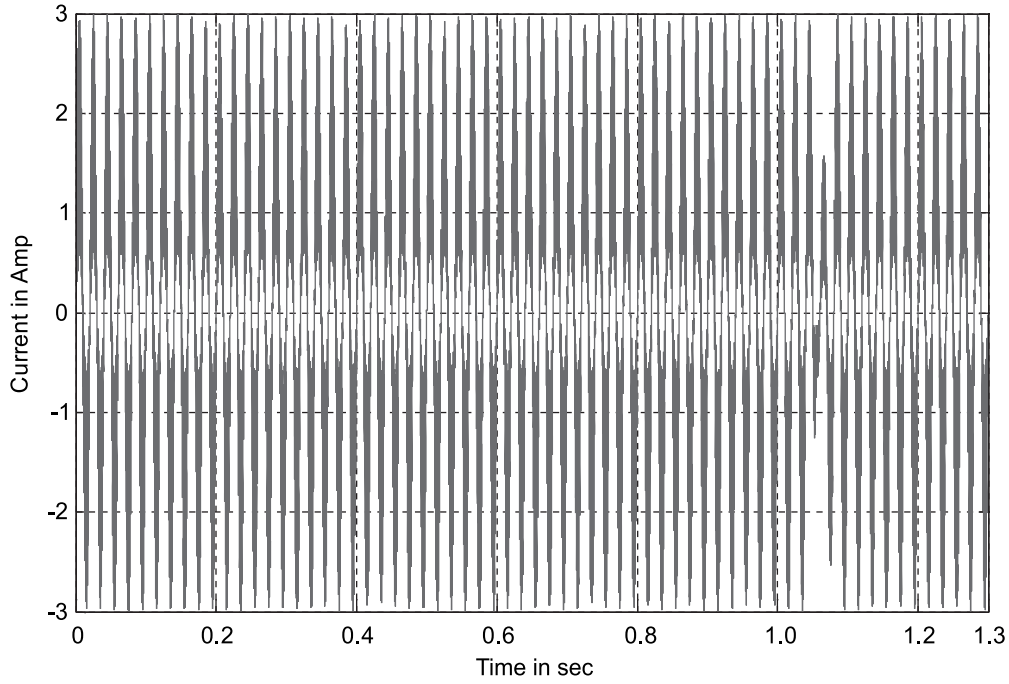


**Figure 4: Current of stator side converter**

## 5. CONCLUSION

The fully controlled type H-Bridge topology was taken for speed control of open ended induction motor. The two side bridges are connected with different voltage levels. The ratio between the two converters excited voltage levels are 1:0.366. The combination of H-Bridge with dodecagonal can reduces stress on power electronic devices in converter and it will reduce losses to a greater extent. The dodecagonal pulse width modulation can suppress the $6n \pm 1$ ($n$ = odd) harmonics completely. The switching harmonics are very less.

## *References*


1. J. Rodriguez, S. Bernet, B. Wu, J. O. Pontt, and S. Kouro, "Multilevel voltage-source-converter topologies for industrial medium-voltage drives," *IEEE Trans. Ind. Electron*., Vol. 54, No. 6, Dec. 2007, pp. 2930-2945.
2. L. G. Franquelo et. al., "The age of multilevel converters arrives", *IEEE Ind. Electron. Magazine*, Vol. 2, No. 2, June 2008, pp. 28-39.
3. J. Rodriguez et. al., "Design and Evaluation Criteria for High Power Drives", Ind. Appl. Society Annual meeting, IAS '08, Oct-2008, pp 1-9.
4. K. K. Mohapatra, K. Gopakumar, V. T. Somasekhar and L. Umanand, "A harmonic elimination and suppression scheme for an open-end winding induction motor drive", *IEEE Trans. Ind. Electron.*, Vol. 50, No. 6, 2003, pp. 1187-1198.
5. S. Lakshminarayanan, G. Mondal, P.N. Tekwani, K.K. Mohapatra and K. Gopakumar, "Twelve-Sided Polygonal Voltage Space Vector Based Multilevel Inverter for an Induction Motor Drive With Common-Mode Voltage Elimination", *IEEE Trans. Ind. Electron*., Vol. 54, No. 5, Oct 2007, pp 2761-2768.
6. Sanjay Lakshminarayanan, R.S. Kanchan, P.N. Tekwani and K.Gopakumar, 'Multilevel inverter with 12 sided polygonal voltage space vector locations for induction motor drive', *IEE Proc.-Electr. Power Application*, Vol. 153, No. 3, May 2006, pp 411-419.
7. A D as, K. Sivakumar, R. Ramchand, C. Patel, and K. Gopakumar, "A combination of hexagonal and 12 sided polygonal voltage space vector PWM control for IM drives using cascaded two-level inverters," *IEEE Trans. Ind. Electron*. Vol. 56, No. 5, pp. 1657-1664, May 2009.
8. Das, K. Sivakumar, R. Ramchand, C. Patel, and K. Gopakumar, "A Pulsewidth Modulated Control of Induction Motor Drive Using Multilevel 12-Sided Polygonal Voltage Space Vectors", *IEEE Trans. Ind. Electron*. Vol. 56, No. 7, pp. 2441-2449, Jul 2009.
9. Das, K. Sivakumar, R. Ramchand, C. Patel, and K. Gopakumar, "A high resolution pulsewidth Modulation technique using concentric multilevel dodecagonal voltage space vector structures", Proc. Conf. Rec. ISIE 2009, pp. 477-482, Jul 2009.
10. K. A. Corzine, M. W. Wielebski, F. Z. Peng and Jin Wang, "Control of cascaded multilevel inverters," *IEEE Trans. Power Electron*., Vol. 19, No. 3, May 2004, pp. 732-738.
11. M. D. Manjrekar, P. K. Steimer, and T. A. Lipo, "Hybrid multilevel power conversion system: a competitive solution for high-power applications", *IEEE Trans. Ind. Appln.*, Vol. 36, No. 3, pp. 834-841, May 2000.
12. Rech and J. R. Pinheiro, "Hybrid multilevel converters: Unified analysis and design considerations", *IEEE Trans. Ind. Electron*., Vol. 54, No. 2, pp. 1092-1104, Apr. 2007.
13. K. Corzine and Y. Familiant, "A new cascaded multilevel H-bridge drive", *IEEE Trans. Power. Electron*., Vol. 17, No. 1, pp. 125-131, Jan. 2002.
14. S. K. Mondal, B. K. Bose, V. Oleschuk and J. O. Pinto, "Space vector pulse width modulation of three level inverter extending operation into over modulation region," *IEEE Trans. Power Electron*., Vol. 18, No. 2, March 2003, pp. 604-611.
15. P. Mcgrath, D. G. Holmes and T. Lipo, "Optimized space vector switching sequences for multilevel inverters", *IEEE Trans. Power Electron*., Vol. 18, No. 6, Nov 2003, pp. 1293-1301.
16. Das, Anandarup, K. Mathew, Chitanpatel, Rijil Ramchand, K.Gopa Kumar, "Dodecagonal Space Vector Diagram Using Cascaded H-Bridge Inverters", *IEEE International Symposium on Industrial Electronics*, 2010.